AUVSAT - an experimental platform for spacecraft formation flying

Thomas R. Krogstad Jan Tommy Gravdahl Kristin Y. Pettersen Even Børhaug
Department of Engineering Cybernetics,
Norwegian University of Science and Technology
N-7491 Trondheim, Norway
thomas.krogstad@itk.ntnu.no

***Abstract*— In this paper we present an experimental platform for relative attitude control of spacecraft. The platform is part of the AUVSAT project at the Norwegian University of Science and Technology, a project with the goal of creating an underwater experimental laboratory for formation control of underwater vehicles and spacecraft. In the following we present the design and the specifications leading to it.**

I. Introduction

The motivation for building an experimental platform is to provide a set-up for experimental verification of theoretical results on spacecraft formation flying demonstrating the strengths and shortcomings of the theory, and in this way contribute to bridge the gap between theory and practice. NTNU has several laboratories for experimental verification of marine control systems, and we wanted to utilize the existing infrastructure when developing the experimental platform for spacecraft formation flying. To this end, we initiated a project to develop an underwater test facility. The facility would consist of two or more autonomous underwater vehicles (AUVs) and three underwater satellites, using an underwater environment and neutrally buoyant vehicles to emulate space.

Examples of existing satellite simulators include the air-bearing platforms described in [3] and [5]. These both use the principle of a balanced platform on a sphere shaped air-bearing, controlled by reaction wheels. Since they balance on a bearing, they have limited travel in pitch and roll. An example of a spacecraft simulator which can rotate freely about all axes, is the IAMBUS [11]. This is a sphere shaped underwater vehicle and was used as a basis for our single vehicle design.

Experimental platforms for spacecraft formation control can also be found in the literature, i.e. the SPHERES project at MIT and the Distributed Spacecraft Attitude Control System Simulator at Virginia Polytechnic Institute and State University [4].

The contribution of this paper is the design of an experimental platform for formation flying of underwater vehicles and spacecraft. In section II we give an introduction to the autonomous underwater vehicles, the focus of this paper is on the spacecraft simulator, and we describe the vehicles and laboratory setup in section III, in section IV we present some theoretical research which will be validated experimentally and finally we give some concluding remarks.

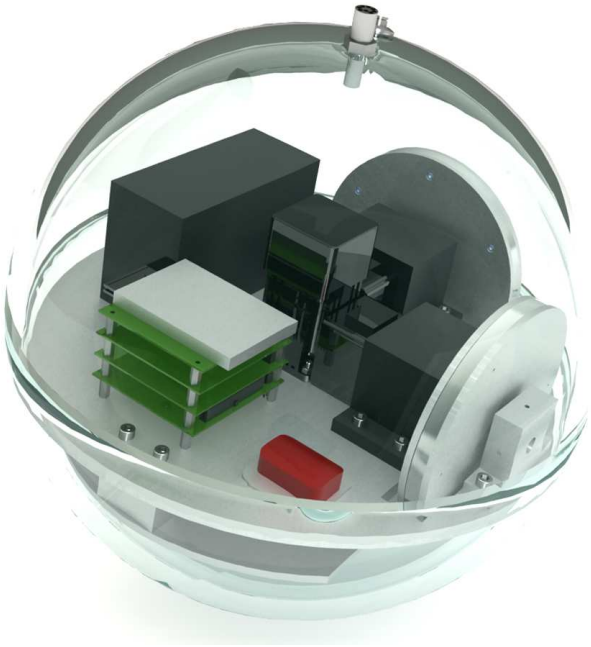

Fig. 1. Computer design of the underwater satellite

II. Autonomous underwater vehicle design

The first stage of the project was the design of two autonomous underwater vehicles. This allowed us to take advantage of prior knowledge at the department. The AUV field is rapidly developing, and several comercial and military vehicles already exist and are applied in numerous tasks, most of which are in the surveillance and survey category. These types of operation requires speed and agility, and most vehicles are therfore shaped to minimize drag and are usually controlled by means of propeller and control surfaces at the rear of the vehicle. With this in mind the design and construction of the Skarv AUV was initiated in 2004 [1] and was finished early 2006 [4] with the vehicle in fig. 2.

However, future AUV operations include inspection and maintenance tasks, where the importance of position keeping will arise. This formed the specifications for the second vehicle of the underwater formation control platform. In the following we give a short summary of the design of this vehicle, the Munin AUV.

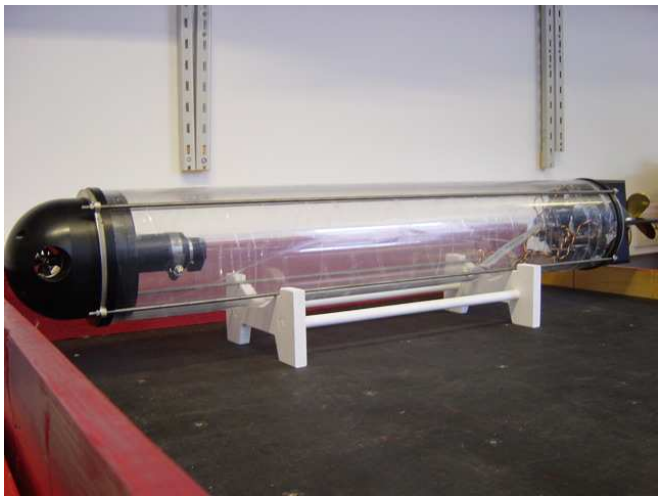

Fig. 2. The Skarv AUV. Here one can clearly see the bow thruster and rear propeller and control planes. The AUV is here shown without control hardware and batteries.

A. Specifications

When designing the second vehicle of the AUV experimental platform, the following set of specifications was chosen to guide the design. Firstly, to keep it small-sized, to be able to operate it in our indoor facilities and to field test it without the need for a lot of equipment and manpower to set it afloat. Secondly, to be maneuverable and able to dynamically position itself accurately in three dimensions. We now show how these guidelines influenced the design.

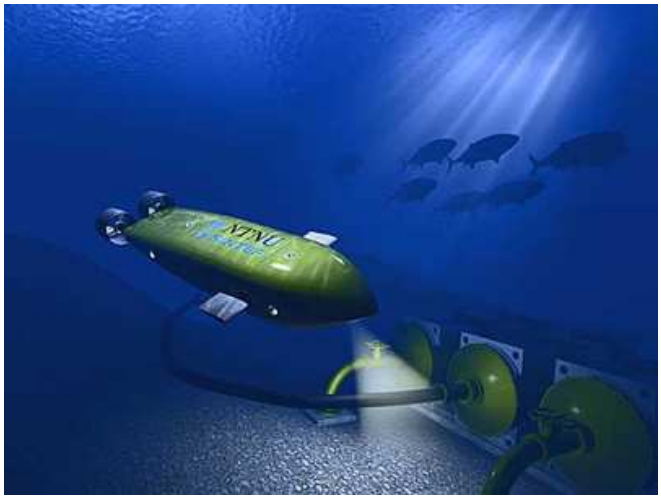

Fig. 3. Illustration of the Munin AUV performing hovering inspection of an offshore oil and gas installation.

B. Hull and construction

The design of Munin's hull had to take both of the previous section's guidelines into consideration. The size and weight of the vehicle were the first factors considered. The length of the vehicle was chosen to be about 1.5 m and the dry-weight had to be no more than 80 kg. This allowed the vehicle to be handled by two persons in the field and during testing. Though the small size of the vehicle made handling simpler, it also meant that even more care would have to be taken when placing internal hardware, and it would complicate maintenance and assembly. To overcome this the hull was sectionized into three compartments; the nose, middle and aft section. In addition to simplifying maintenance and assembly, it also gives flexibility to extend the vehicle by additional sections to include more sensors, battery power, actuators etc.

To add maneuverability the hull would include 4 tunnel thrusters, as well as feedthroughs for propeller and dive plane shafts.

To simplify construction, the basic structure of each section was first shaped in high density polyurethane foam. This material is typically used in architectural modeling and prototyping, and is easily shaped to the desired profiles. The basic structure was then hollowed out to shape the internal compartments, and holes for feedthroughs and thrusters were drilled and reinforced using acrylic piping. The remaining foam shell wash then covered in glassfibre reinforced plastics to add strength and waterproofness.

C. Sensors

Due to the three compartment design and simple assembly and disassembly procedure, the AUV has the flexibility to include a large number of different sensors, both for navigation and for mission-dependent measurement purposes. Currently the AUV is equipped with sensors measuring attitude, depth and surface position. The attitude sensor is the low-cost MEMS inertial measurement unit (IMU) Xsens MTi, chosen for its ease of use, small-size and prior utilization in underwater vehicles. The depth is measured using a Tecsis pressure sensor. Additionally a Garmin GPS antenna is included to provide position measurements while surfaced. Moreover, it can provide absolute position estimate updates when using navigation grade IMUs to integrate position while operating underwater. Navigation grade refers to the amount of drift in position and attitude estimates obtained from accelerometer and gyro measurements.

Planned enhancements of the design include an additional section, including a Teledyne Explorer doppler velocity log (DVL) and a Kongsberg Seatex MRU, to provide more accurate position and velocity estimates during diving. Furthermore, a sonar will be incorporated to provide more accurate depth and bottom profiling.

D. Actuators

To satisfy the hoovering requirement and as mentioned in the hull design section, the AUV is actuated by means of tunnel thrusters, propellers and dive planes. For low-speed positioning and attitude control, two pairs of vertical and horizontal tunnel thrusters are used in conjunction with two rear propellers. At higher speeds the tunnel thrusters are less efficient, and the depth is instead controlled using the dive planes while the heading is controlled by running the rear propellers differentially.

The tunnel thrusters are powered by Maxon RE35 DC motors, providing 130 Watts of power, while the dive planes are controlled by two HiTec metal gear mini servos.

III. Underwater satellite design

In this section we present the design of the spacecraft simulator part of the underwater experimental platform, and the specifications which lead up to the final design. The motivation for our design came from the need to experimentally verify theoretical results on spacecraft control, and in particular verify control schemes for relative attitude control in spacecraft formations.

TABLE I
HARDWARE OVERVIEW FOR THE UNDERWATER SATELLITES

Device	Name	Description
Actuators		
Motor	SmartMotor SM2330D	Compact servo motor with integrated motor control hardware
Ballast system	XP250-12 Piston Tank	This is a piston operated ballast system, capable of adjusting the mass of the vehicle by 250 g.
Main control computer		
PC/104 CPU card	Kontron MOPSlcdLX	Main board with 500MHz Pentium processor and 1 GB RAM
PC/104 Serial communication extension card	Xtreme-4/104	4 extra 16C654 UARTS, RS232/RS485 connections
PC/104 IO card	Access 104-AIO12-8	Analog and digital inputs and outputs.
Power supply	HESC104 Vehicle power supply	Powers the PC/104 stack and also has additional power connections for sensors and piston tank control motor.
Solid state storage	FlashDrive/104	4GB of flash storage

TABLE II
SENSOR PROPERTIES

Sensor	Property	Accuracy
XSens MTi	Angular resolution	0.05 deg
	Static accuracy (Roll/Pitch)	< 0.05 deg
	Static accuracy (Heading)	< 1 deg
	Dynamic accuracy	2 deg RMS
Pressure sensor	Range	0-1 bar
	Accuracy	0.01 m

A. Hull design

The design of the hull was based on a need to minimize drag and other hydrodynamic effects, and to have a hull which made it easier to achieve a center of mass coinciding with the center of buoyancy. The decision to make the hull spherical therefore seemed sensible. Several options where considered, aluminum and glass-fibre reinforced plastics were some which were later discarded. Due to space-requirements of actuators, sensors and control hardware, the internal space required for the system suggested an diameter of 30-40 cm. The side-effect of this design choice is that the sphere creates a lot of buoyancy, to help counter this the material of the pressure hull should be dense. In addition the material could not have properties which interfered with magnetometer measurements. The choice finally fell on an 17" spherical glass instrument housing. This instrument housing, manufactured by Nautilus Marine Service GmbH, is typically used in deep sea research, and has precision cut mating edges. This enables the sphere to be kept closed by evacuating air through a pressure vent, requiring no exterior mechanical device to close the spheres, keeping the surface streamlined.

B. Sensors

Due to space restrictions, the low-cost and small-size Xsens MTi IMU was also chosen for the spacecraft simulator. This sensor uses three-axis gyro and magnetometer data to obtain attitude and angular velocity. The accuracy and noise ratio is provided in table II. The sensor and vehicle computer communicates through a serial connection. The sensor can be programmed to send data at different rates from on-demand to 100 Hz, which is sufficient for our use. The sensor can also send the attitude data as quaternions, Euler angles or as a direction cosine matrix, and can also provide the actual magnetometer data which can be convenient to simulate typical student-made cubesats, where the only sensors typically are magnetometers [8].

In addition to the IMU, we also have a pressure sensor. This is used when controlling the vertical position of the vehicles, to keep them fully submerged during experiments. We do not control the horizontal position position in this setup. But since we will do experiments in an indoor pool, the horizontal position should be relatively stable and collisions can be avoided provided the initial distances between vehicles are kept large enough.

C. Actuators

To minimize drag and get experience with spacecraft related actuators, it was decided to internally actuate the vehicle using reaction wheel assemblies. Each vehicle has three assemblies mounted orthogonally along the x,y and z body axes. The reaction wheel assembly consists of an aluminum and lead momentum wheel, mounted to a servo motor. The servo motor is controlled to store and deliver momentum to the wheel. Three factors were considered when selecting the motor: size, torque and speed. Size was limited by the internal volume of the sphere, consequently limiting the maximum possible speed and torque. Moreover, torque and speed are competing features, i.e. by demanding high torque, the maximum speed is reduced and vice versa. In our case two factors dictated the choice of parameters. The

top speed of the motor and inertia of the momentum wheel determines the amount of momentum which can be stored and hence, how long we can operate the vehicle before dumping momentum. The maximum torque determines the restoring moment which can be suppressed. The latter factor was deemed most important, as the inability to suppress the restoring moments would render the vehicle inoperable. Using an mathematical model of the vehicle, we did calculations and simulations to conclude. The choice was the Animatics SM2330 servomotor.

D. Communication

Communication with the vehicles are done using Ethernet LAN. Each vehicle sends sensor information to a server, and asks for sensor data from the other vehicles. Future extensions of the platform include researching the use of radio frequency or acoustic communication to communicate wirelessly while submerged.

E. Main computer

The main computer comprises PC/104 embedded computer boards, containing CPU motherboard, IO communication card, power supply card, serial communication extension card and solid state storage. The PC/104 form factor is a compact implementation of the PC bus as found in a desktop computer, but implemented on modular and stackable circuit boards. The standard was developed to alleviate the need for specially developed PC boards in embedded applications requiring the abilities of the desktop PC bus. The CPU board has a 500 MHz low power Pentium processor and 1 GB of RAM, which is more than sufficient for this application. The system has 4 GB of solid state storage, sufficient for OS requirements, main programs and data storage. The IO communication card carries digital and analog input and output cards to communicate with sensors.

F. Software design

The software was designed to be used in both the AUVs and the spacecraft simulators. Therefore the software needed to be reusable and easy to maintain, keeping most vehicle specific code in low-level drivers. Implementation and design of control schemes should also be straightforward and intuitive. In addition the system needed to communicate with low-level hardware (sensors, actuators, communication devices, etc.) in a reliable and timely manner. In what follows we give a short description software used to satisfy these specifications.

1) Vehicle operating system: In control systems, the ability to communicate with sensors and actuators in real-time is of the utmost importance. i.e. we need to handle incoming sensor data, make it available to the control algorithm and send the resulting command to the actuators with as little delay as possible. An operating system which satisfies these demands is therefore called a real-time operating system (RTOS). The QNX Neutrino is such a RTOS, in addition to being specifically designed for embedded systems. It is microkernel-based, i.e. the operating system is run as a number of small tasks or servers. The advantage is a very scalable OS, in that by shutting down features which are unnecessary it can be implemented in a very compact form advantageous for system with limited resources. It also includes real-time features such as task prioritizing and scheduling, and intertask communication and resource sharing.

2) Matlab Real-time workshop: To facilitate rapid prototyping and implementation of control laws, we are using Matlab real-time workshop in combination with Simulink. Real-time Workshop is a Matlab toolbox which is used to generate C source code, which can be compiled and run on the target QNX computer in addition to provide a communication interface between the program run on the target computer and the Simulink program on the host. This makes it possible to graphically represent measurements and control signals in real-time in Simulink, and to log data for later analysis.

3) Simulink: Another advantage of using Matlab Real-time workshop, is the integration with the Simulink development environment. It has a graphical user interface, where dynamical models and algorithms are created by placing function blocks (i.e integrators, derivatives, gains, etc.) This also means that we can easily change between simulation and hardware implementation by just moving the block containing the control algorithm, provided we ensure that the two models contain equivalent inputs and outputs.

4) Low level interfaces: As we are using devices which for the most part do not have readily available QNX drivers, these have been developed by our team. The drivers were written in c programming language and compiled as shared libraries, in this way they would not need to be compiled over again when the main program was changed.

G. Internal structure

The hardware components are mounted on a solid aluminum framework, to keep the system from vibrating, as shown in fig. 1. The reaction wheel assemblies are mounted orthogonal to each other along the body axes. In addition to the required hardware, lead weights were calculated and placed both to make the vehicle neutrally buoyant and to achieve a center of gravity coinciding with the center of buoyancy.

IV. Formation control

As previously noted, the main objective when designing the platform, was to provide a set-up for experimental verification of theoretical results on spacecraft formation flying demonstrating the strengths and shortcomings of the theory, and in this way contribute to bridge the gap between theory and practice. In this section we will present related theoretical work in the field of relative attitude control of formation flying spacecraft.

A. Mathematical model

We divide the mathematical model of the spacecraft equations of motion into two parts: the kinematic and dynamical

model. The kinematic model relates the rotation of the spacecraft to its angular velocities in the space SO(3), while the dynamical or kinetic model relates angular velocity to internal and external moments or torques.

The kinematic differential equation is in its most general form given by

$$\dot{\mathbf{R}}_i^b = (\boldsymbol{\omega}_{bi}^b)^\times \mathbf{R}_i^b = -(\boldsymbol{\omega}_{ib}^b)^\times \mathbf{R}_i^b, \tag{1}$$

where $\boldsymbol{\omega}_{bi}^b$ is the angular velocity of the body frame $\mathcal{F}_b$ with respect to the inertial frame $\mathcal{F}_i$, and $\mathbf{R}_i^b$ is the rotation matrix between frames. A frame is a 3-axis orthogonal coordinate system. $^\times$ denotes the vector cross product operator. Typically a parametrization of SO(3) is used, examples of such include Euler angles, unit quaternion and Rodriguez-parameters. In the controller we present here we have utilized the unit quaternion, or Euler parameters which they are also often called. The advantage of this representation, and the reason why it has grown popular in space related control algorithms, is that it is non-singular. Meaning that for any given orientation the kinematic differential equation always has a valid solution. In the unit quaternion formulation the kinematic differential equations are expressed as

$$\dot{\eta}_{ib} = -\tfrac{1}{2}\boldsymbol{\epsilon}_{ib}^T \boldsymbol{\omega}_{ib}^b \tag{2a}$$
$$\dot{\boldsymbol{\epsilon}}_{ib} = \tfrac{1}{2}[\eta_{ib}\mathbf{I} + \boldsymbol{\epsilon}_{ib}^\times]\boldsymbol{\omega}_{ib}^b, \tag{2b}$$

The dynamical model of a spacecraft internally actuated by means of reaction wheels, is often referred to as a gyrostat model, and the details of its derivation can be found in [2] or [6]. The model is given by

$$\mathbf{J}\dot{\boldsymbol{\omega}}_{ib}^b = (\mathbf{J}\boldsymbol{\omega}_{ib}^b)^\times \boldsymbol{\omega}_{ib}^b + (\mathbf{A}\mathbf{I}_s\boldsymbol{\omega}_s)^\times \boldsymbol{\omega}_{ib}^b - \mathbf{A}\boldsymbol{\tau}_a + \boldsymbol{\tau}_e \tag{3a}$$
$$\mathbf{I}_s\dot{\boldsymbol{\omega}}_s = \boldsymbol{\tau}_a - \mathbf{I}_s\mathbf{A}\dot{\boldsymbol{\omega}}_{ib}^b, \tag{3b}$$

where $\mathbf{A} \in \mathbb{R}^{3\times 4}$ is a matrix of wheel axes in $\mathcal{F}_b$ given by, [12],

$$\mathbf{A} = \begin{bmatrix} \sqrt{\frac{1}{3}} & \sqrt{\frac{1}{3}} & -\sqrt{\frac{1}{3}} & -\sqrt{\frac{1}{3}} \\ \sqrt{\frac{2}{3}} & -\sqrt{\frac{2}{3}} & 0 & 0 \\ 0 & 0 & -\sqrt{\frac{2}{3}} & \sqrt{\frac{2}{3}} \end{bmatrix}, \tag{4}$$

$\mathbf{I}_s \in \mathbb{R}^{4\times 4}$ a diagonal matrix of wheel axial inertias, $\boldsymbol{\omega}_s \in \mathbb{R}^4$ a vector of wheel velocities and $\mathbf{J} \in \mathbb{R}^{3\times 3}$ the total moment of inertia.

B. Control algorithms

In our work we have focused on a leader-follower synchronization strategy. In this control scheme we assume that the leader spacecraft is controlled by some stable controller, and design a controller for the follower such that the orientation and angular velocity are synchronized to those of the leader [7].

We first define an error variable or synchronization measure relating the attitudes of the leader and follower

$$\mathbf{q}_{se} \triangleq \mathbf{q}_{lf} = \mathbf{q}_{li} \otimes \mathbf{q}_{if} = \mathbf{q}_{il}^{-1} \otimes \mathbf{q}_{if}, \tag{5}$$

while the angular velocity synchronization error is equal to the relative velocity,

$$\boldsymbol{\omega}_{se} \triangleq \boldsymbol{\omega}_{lf}^f = \boldsymbol{\omega}_{if}^f - \mathbf{R}_l^f \boldsymbol{\omega}_{il}^l. \tag{6}$$

Given the error-variables (5) and (6), the error-dynamics may be represented by

$$\begin{aligned}\mathbf{J}\dot{\boldsymbol{\omega}}_{se} = {} & (\mathbf{J}\boldsymbol{\omega}_{if}^f + \mathbf{A}\mathbf{I}_s\boldsymbol{\omega}_{s,f})^\times \boldsymbol{\omega}_{if}^f - \mathbf{A}\boldsymbol{\tau}_{a,f} + \boldsymbol{\tau}_{g,f} \\ & - \mathbf{J}(\boldsymbol{\omega}_{se})^\times \mathbf{R}_l^f \boldsymbol{\omega}_{il}^l - \mathbf{J}\mathbf{R}_l^f \dot{\boldsymbol{\omega}}_{il}^l \end{aligned} \tag{7a}$$
$$\dot{\mathbf{q}}_{se} = \tfrac{1}{2}\mathbf{Q}(\mathbf{q}_{se})\boldsymbol{\omega}_{se}, \tag{7b}$$

where the subscripts f on $\boldsymbol{\tau}_{a,f}$ and $\boldsymbol{\tau}_{g,f}$, is to clearly distinguish between leader and follower torques.

Proposition 1. *The error-dynamics* (7)*, with control input given by*

$$\begin{aligned}\boldsymbol{\tau}_{a,f} = -\mathbf{A}^\dagger \Big\{ & -(\mathbf{J}\boldsymbol{\omega}_{if}^f + \mathbf{A}\mathbf{I}_s\boldsymbol{\omega}_{s,f})^\times \mathbf{R}_l^f \boldsymbol{\omega}_{il}^l - \boldsymbol{\tau}_{g,f} \\ & + \mathbf{J}(\boldsymbol{\omega}_{se})^\times \mathbf{R}_l^f \boldsymbol{\omega}_{il}^l + \mathbf{J}\mathbf{R}_l^f \dot{\boldsymbol{\omega}}_{il}^l \\ & - k_d\boldsymbol{\omega}_{se} + k_p sgn(\eta_{se})\boldsymbol{\epsilon}_{se} \Big\}, \end{aligned} \tag{8}$$

have a uniformly globally asymptotically stable origin $(\boldsymbol{\omega}_{se}, \mathbf{y}) = (\mathbf{0}, \mathbf{0})$*, where* $\mathbf{y} \triangleq col(1 - |\eta_{se}|, \boldsymbol{\epsilon}_{se})$

Proof. The proof is conducted using an extension om Matrosov's Theorem [10] given in, [9], and can be found in [7]. □

C. Simulations

In this chapter we show some simulations of leader-follower synchronization, to indicate the kind of motion we want to recreate using the underwater satellite simulator. The initial conditions are given in table IV

The model used is based on realistic values for a cubic small-size satellite, and a summary of model parameters is given in Table III.

TABLE III
MODEL PARAMETERS

Parameter	Value
Inertia matrix	$\text{diag}\{4, 4, 3\}$ $[kgm^2]$
Wheel inertia	$8 \cdot 10^{-3}$ $[kgm^2]$
Max magnetic moment	40 $[Am^2]$
Max wheel torque	0.2 $[Nm]$
Max wheel speed	400 $[rad/s]$

TABLE IV
SIMULATION PARAMETERS

Parameter	Value
Controller gains	$k_p = 1$, $k_d = 5$
Desired pointing accuracy	0.1° in all axes
Orbit angular velocity	$1.083 \cdot 10^{-3}$ $[rad/s]$
Initial leader attitude	$[0, 0, 0]^T$ $[Deg]$
Initial follower attitude	$[20, 20, 0]^T$ $[Deg]$

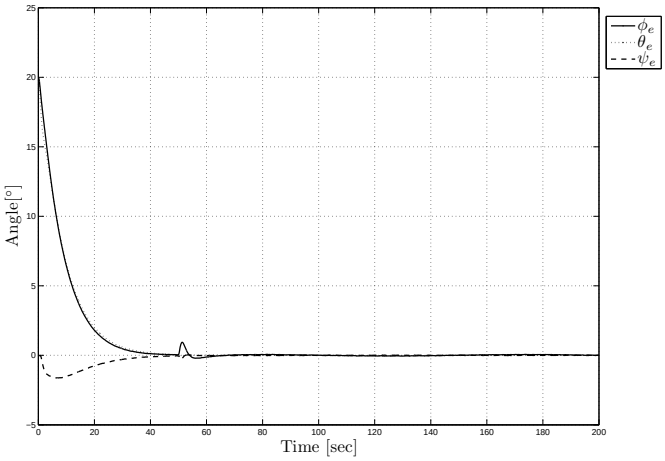

Fig. 4. Synchronization error transient $\mathbf{q}_{se}$, visualized in Euler angles.

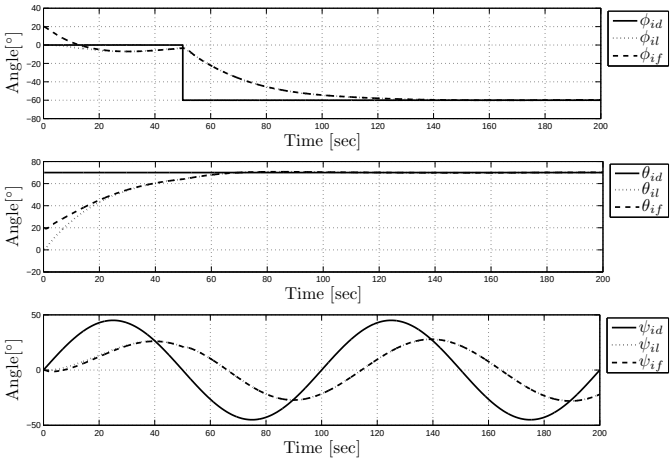

Fig. 5. Simulation plot showing the attitude of the leader and follower versus the desired attitude.

In fig. 4 a plot of the transient synchronization error is presented, clearly showing the asymptotic convergence. In fig. 5 it is shown how the follower tracks the attitude of the leader.

V. CONCLUSION

In this paper we have presented an experimental platform for relative attitude control of formation flying spacecraft, using internally actuated underwater vehicles. We have also given a short introduction to the AUVSAT project, where this satellite platform is an integral part.

Fig. 6. Animatics SmartMotor SM2330D

Fig. 7. Tecsis pressure sensor and XSens IMU. The battery is of size AAA

Fig. 8. Piston tank for the ballast system

Fig. 9. PC/104 embedded computer

REFERENCES

[1] E. Børhaug. Cross-track maneuvering and way-point tracking control of underactuated auvs in particular and mechanical systems in general. Master's thesis, Norwegian University of Science and Technology, 2005.

[2] C. D. Hall. Spinup dynamics of gyrostats. *Journal of Guidance, Control, and Dynamics*, 18(5):1177–1183, Sptember-October 1995.

[3] D. Jung and P. Tsiotras. A 3-dof experimental test-bed for integrated attitude dynamics and control research. In *AIAA Guidance, Navigation and Control Conference*, 2003.

[4] S. A. Kowalchuk and C. D. Hall. Distributed spacecraft attitude control simulator: Feedback control capabilities and visualization techniques. In *7th International Symposium on Quantitative Feedback Theory (QFT) and Robust Frequency Domain Design Methods*, 2005.

[5] S. A. Kowalchuk and C. D. Hall. Hardware-in-the-loop simulation of classical element feedback controller. In *Flight Mechanics Symposium*, NASA Goddard Space Flight Center, Greenbelt, Maryland, 2005.

[6] T. R. Krogstad. Attitude control of satellites in clusters. Master's thesis, Norwegian University of Science and Technology, 2005.

[7] T. R. Krogstad, J. T. Gravdahl, and R. Kristiansen. Coordinated control of satellites. In *Proceedings of the 2005 International Astronautical Congress*, October 2005.

[8] T. R. Krogstad, J. T. Gravdahl, and P. Tondel. Explicit model predictive control of a satellite with magnetic torquers. In *2005 IEEE International Symposium on Intelligent Control and 13th Mediterranean Conference on Control and Automation, Jun 27-29 2005*, pages 491–496, 2005.

[9] A. Loria, E. Panteley, D. Popovic, and A. Teel. An extension of matrosov's theorem with application to stabilization of nonholonomic control systems. In *Proceedings of the 41st IEEE Conference on Decision and Control*, volume 2, pages 1528–1533, December 2002.

[10] V. M. Matrosov. On the stability of motion. *Journal of Appl. Math. Mech.*, 26:1337–1353, 1962.

[11] C. Schultz and C. A. Woolsey. An experimental platform for validating internal actuator control strategies. In *Proc. 1st IFAC Workshop on Guidance & Control of Underwater Vehicles*, 2003.

[12] R. Wisniewski. Lecture notes on modeling of a spacecraft. [Available online:www.control.auc.dk/ raf/ModellingOfMech/Rep8sem.ps, Last accessed: 05.06.2005], May 2000.